Optical properties of excitons in semi-infinite semiconductors

A. D'Andrea
Istituto di Metodologie Avanzate Inorganiche del Consiglio Nazionale delle Ricerche, Montelibretti, Italy

R. Del Sole
Dipartimento di Fisica, Seconda Università degli Studi di Roma, Tor Vergata, I-00173 Roma, Italy
(Received 19 October 1987)

We start from a microscopic model, previously developed by the authors, of excitons in semi-infinite semiconductors. The model allows the determination in closed form of the nonlocal exciton polarizability from wave functions. This embodies the additional boundary condition and a transition layer, whose depth is smaller than the exciton radius, where the exciton polarizability varies from the vacuum to the bulk value. Here we show how to calculate in closed form within the microscopic model non-normal incidence reflectivity, surface-polariton dispersion, and attenuated total reflection. The comparison between theory and experiments shows good agreement in several materials, while some discrepancies are found in InP and GaAs.

I. INTRODUCTION

Although it is now three decades since the fundamental problem of exciton reflectivity was addressed in the pioneering work by Pekar,[1] a generally accepted solution is not yet available. The situation is complicated by two different—yet concurrent—effects, i.e., the spatial dispersion of the exciton polarizability and the surface potential. The former, arising from the finite value of the exciton mass M, generates two polariton branches, whose relative amplitude is determined by the so-called additional boundary condition (ABC). The latter effect, which occurs even if M is infinite, arises from the finite extent of the exciton wave function, that leads to a repulsive surface potential and therefore to the dead-layer effect.[2] While much work has been done involving macroscopic models of the dead layer and *ad hoc* assumptions of ABC,[3] it is now clear that both the dead layer and the ABC (and their relation) can be derived from the knowledge of exciton wave functions in the semi-infinite semiconductor.[4,5] It is the exciton behavior near the surface, i.e., the surface potential, that determines the ABC.

Most of the work on exciton wave functions has been made assuming the no-escape boundary condition[5] that implies the vanishing of the wave function when either the electron or the hole is at the surface. Such a boundary condition can be derived from general arguments, and has been shown to hold at least when near-gap surface states are not present,[6] as is the case for surfaces not held in ultrahigh vacuum, where dangling bonds are usually saturated by air molecules. It also seems reasonable to neglect the image potential, which repels electrons and holes from the surface, since this effect has already been accounted for—yet partially—by the boundary condition. Within this framework, the present authors have given a numerical solution of the effective-mass exciton equation, based on a variational method of fulfilling the boundary conditions.[5,7] A different approach, based on the adiabatic separation of the light-mass relative motion from the slow center-of-mass motion,[8,9] leads to nearly identical wave functions, provided that a very accurate solution of the light-mass problem is carried out.[7] The beautiful agreement between these independent approaches confirms the validity of both.

The numerical wave functions computed in Ref. 7 can be well reproduced by analytical wave functions involving a fitting parameter, allowing the analytical calculation of the nonlocal dielectric susceptibility of the vacuum-semiconductor system.[7] A transition layer (roughly speaking, the dead layer) is present below the surface, where the exciton contribution to the dielectric function, starting from zero at the surface, is smaller than in the bulk. The transition-layer depth depends on the mass ratio m_e/m_h and is slightly smaller than the exciton radius a_B. After this layer, the dielectric function is given [in terms of the bulk dielectric function $\epsilon_b(z-z')$] by

$$\epsilon(z,z')=\epsilon_b(z-z')+U\epsilon_b(z+z')$$

as hypothesized in Ref. 3. The weight U of the specularly reflected term turns out to be dependent on frequency, dead-layer depth, and on other exciton parameters,[5,10] in contrast with simpler expressions resulting from the assumed ABC's.[3] This work has pointed out for the first time the connection between the ABC and the dead layer.

In this paper we address the following question: is the present model of excitons in semi-infinite semiconductors (based on the no-escape boundary condition and on the neglect of the image potential) realistic enough to describe optical experiments in real semiconductors? Answering this question will shed some light on the importance of extrinsic dead layers (arising, for instance, from built-in electric fields), and on the reason why previous estimates of the dead layer were more than twice larger than the present result. Furthermore, we would like to investigate the validity of the three-layer model (where a homogeneous dead layer is assumed) with respect to our results.

In order to answer these questions we use the nonlocal dielectric susceptibility obtained from our wave functions to predict the results of a number of experiments: s and p reflectivities, their phase difference, the relative populations of lower- and upper-polariton branches, surface polariton dispersion, and attenuated total reflection (ATR). The results of our calculations are compared with those based on Pekar's ABC (which is the most similar to ours) with or without a homogeneous dead layer, and with experimental data when available. Our approach in this work is not to adjust exciton parameters in order to reproduce closely a single experiment, but rather to use the same set of parameters, mostly taken from the literature, to give a reasonable account of many experiments. We find that our calculations reproduce fairly well experimental data in several cases, showing that extrinsic dead layers should not be important there. However, in the case of GaAs and InP some features of the experimental spectra cannot be reproduced by the present microscopic model.

In Sec. II A we summarize the equations describing s-wave reflectivity, already derived elsewhere;[5] in Sec. II B we derive the equations describing p-wave reflectivity. In Sec. III we treat surface polaritons and ATR. The reader who is not interested in the mathematical developments can jump directly to Sec. IV, where the results obtained for normal- and oblique-incidence reflectivity and ATR are discussed and compared with experiments. Here we also discuss the phase difference between s and p reflectivities and the relative population of upper- and lower-polariton branches. The conclusions of this work are summarized in Sec. V.

II. THEORY OF REFLECTIVITY

In this section we give the expressions of s and p reflectivities, derived from the nonlocal dielectric function

$$\epsilon(k_{\parallel},z,z')=\epsilon_0\delta(z-z')+(i4\pi\alpha M_{\perp}\omega_0/2\hbar q)\times\{\exp(iq\,|z-z'|)+U\exp[iq(z+z')]-2q[\exp(iqz-Pz')+\exp(iqz'-Pz)-\exp(-Pz-Pz')]/(q-iP)\} \quad (1)$$

that has been obtained starting from the exciton wave functions.[5,7] Here $M_{\parallel}$ and $M_{\perp}$ are the exciton masses in the directions parallel and perpendicular to the surface, $\hbar\omega_0$ is the exciton energy at $\mathbf{k}=0$, P is the inverse transition-layer depth,

$$q=[2M_{\perp}(\hbar\omega-\hbar\omega_0+i\Gamma)/\hbar^2-k_{\parallel}^2M_{\perp}/M_{\parallel}]\,, \quad (2)$$

$U=(q+iP)/(q-iP)$ and Γ is the exciton lifetime broadening.

A. s reflectivity

The s-wave reflectivity has been computed in Ref. 5. Here we restate the result for the sake of completeness, in a slightly different form, using the concept of surface impedance.

We consider s light polarized in the y direction, propagating within the xz plane. The electric field inside the crystal ($z>0$) is[5]

$$\mathcal{E}_y(x,z)=\sum_{i=1}^{2}\mathcal{E}_i\left[e^{iq_iz}+\frac{2P(P^2+q^2)}{(q_i^2-q^2)(P-iq_i)}e^{-Pz}\right]e^{ik_{\parallel}x}\,. \quad (3)$$

Let us define the new quantities:

$$\gamma_1=1\,, \quad (4)$$

$$\gamma_2=(\mathcal{E}_2/\mathcal{E}_1)=-\frac{(q_2^2-q^2)(P-iq_2)(q_1-q-\gamma)}{(q_1^2-q^2)(P-iq_1)(q_2-q-\gamma)}\,, \quad (5)$$

with

$$\gamma=(q+iP)\{(2P/B)(P+iq)[\epsilon_0(\omega^2/c^2)+P^2-k_{\parallel}^2]-1\}\,, \quad (6)$$

$$B=(\omega^2/c^2)4\pi\alpha M_{\perp}\omega_0/\hbar\,. \quad (7)$$

The reflectivity can be obtained, in terms of the s-wave impedance

$$Z_s\equiv\mathcal{E}_y(x,0^+)/H_x(x,0^+)=-(\omega/c)\frac{\sum_{i=1}^{2}\gamma_i\left[1+\frac{2P(P^2+q^2)}{(q_i^2-q^2)(P-iq_i)}\right]}{\sum_{i=1}^{2}\gamma_i\left[q_i+\frac{2P^2(P^2+q^2)}{(q_i^2-q^2)(P-iq_i)}\right]}\,, \quad (8)$$

from the continuity of the electric and magnetic fields at the surface. Writing the vacuum electric field as

$$\mathcal{E}_y(x,z)=[\exp(ik_zz)+r_s\exp(-ik_zz)]e^{ik_{\parallel}x}\,, \quad (9)$$

with $k_z=(\omega/c)\cos\vartheta$, ϑ being the angle of incidence, we obtain the reflectivity amplitude as

$$r_s=-(1+ck_zZ_s/\omega)/(1-ck_zZ_s/\omega)\,. \quad (10)$$

B. p reflectivity

We seek solutions of Maxwell's equations with the electric field parallel to the plane of incidence (xz). It can be written in the form

$$\mathcal{E}_{\alpha}(x,z)=E_{\alpha}(z)\exp(ik_{\parallel}x)\quad(\alpha=x,y,z)\,. \quad (11)$$

We take E_x and E_z different from zero, but $E_y=0$. Inserting $\mathcal{E}_{\alpha}(x,z)$ and the nonlocal dielectric function (1) into Maxwell's equations, we obtain

$$ik_{\parallel}\frac{\partial E_x}{\partial z}+\left[k_{\parallel}^2-\epsilon_0\frac{\omega^2}{c^2}\right]E_z-iB\int_0^{\infty}dz'\exp(iq\,|z-z'|)E_z(z')/(2q)-\bar{\gamma}\exp(iqz)-\delta\exp(-Pz)=0\,, \quad (12a)$$

$$ik_{\parallel}\epsilon_0 E_x+\epsilon_0\frac{\partial E_z}{\partial z}-k_{\parallel}B(c^2/\omega^2)\int_0^{\infty}dz'E_x(z')\exp(iq\mid z-z'\mid)/(2q)$$
$$+iB(c^2/\omega^2)\frac{\partial}{\partial z}\int_0^{\infty}dz'E_z(z')\exp(iq\mid z-z'\mid)/(2q)-\eta\exp(iqz)-\theta\exp(-Pz)=0\ . \tag{12b}$$

Here θ, η, $\bar{\gamma}$, and δ are the following integrals:

$$\theta=B[(c^2/\omega^2)/(q-iP)]\int_0^{\infty}dz'[k_{\parallel}E_x(z')+iPE_z(z')][\exp(-Pz')-\exp(iqz')]\ , \tag{13}$$

$$\eta=B\{(c^2/\omega^2)/[2q(q-iP)]\}\int_0^{\infty}dz'[k_{\parallel}E_x(z')+qE_z(z')][(q+iP)\exp(iqz')-2q\exp(-Pz')]\ , \tag{14}$$

$$\bar{\gamma}=\{iB/[2q(q-iP)]\}\int_0^{\infty}dz'E_z(z')[(q+iP)\exp(iqz')-2q\exp(-Pz')]\ , \tag{15}$$

$$\delta=iB\int_0^{\infty}dz'E_z(z')[\exp(-Pz')-\exp(iqz')]/(q-iP)\ , \tag{16}$$

and the quantities q and B are defined in (2) and (7), respectively. If we operate on both equations (12) with the differential operator $(q^2+\partial^2/\partial z^2)$,[4] we obtain two coupled differential equations:

$$ik_{\parallel}\left[\frac{\partial^2}{\partial z^2}+q^2\right]\frac{\partial E_x}{\partial z}+\left[\left[k_{\parallel}^2-\epsilon_0\frac{\omega^2}{c^2}\right]\frac{\partial^2}{\partial z^2}+q^2\left[k_{\parallel}^2-\epsilon_0\frac{\omega^2}{c^2}\right]+B\right]E_z=(P^2+q^2)\delta\exp(-Pz)\ , \tag{17a}$$

$$ik_{\parallel}\left[\epsilon_0\frac{\partial^2}{\partial z^2}+\epsilon_0q^2-B\frac{c^2}{\omega^2}\right]E_x+\left[\epsilon_0\frac{\partial^2}{\partial z^2}+\epsilon_0q^2-B\frac{c^2}{\omega^2}\right]\frac{\partial E_z}{\partial z}=(P^2+q^2)\theta\exp(-Pz)\ . \tag{17b}$$

The solution of this system is

$$E_{\alpha}(z)=\sum_{i=1}^{3}\mathcal{E}_i^{\alpha}\exp(iq_iz)+\mathcal{E}_p^{\alpha}\exp(-Pz)\quad(\alpha=x,z) \tag{18}$$

where $\mathcal{E}_p^{\alpha}\exp(-Pz)$ is a particular solution of the nonhomogeneous system, with

$$\mathcal{E}_p^z=\left[P\left[\epsilon_0-B\frac{c^2}{\omega^2}/(P^2+q^2)\right]^{-1}\theta+\delta\right]\Big/\left[k_{\parallel}^2-P^2-\frac{\omega^2}{c^2}\epsilon_0+\frac{B}{P^2+q^2}\right]\ , \tag{19a}$$

$$\mathcal{E}_p^x=\frac{i}{k_{\parallel}P}\left[\delta-\left[k_{\parallel}^2-\epsilon_0\frac{\omega^2}{c^2}+\frac{B}{P^2+q^2}\right]\mathcal{E}_p^z\right]\ . \tag{19b}$$

The first term in (18) is the general solution of the homogeneous system, where the wave vectors q_i are those of bulk polaritons, given by the equation

$$\left[\epsilon_0(q_i^2-q^2)+B\frac{c^2}{\omega^2}\right]\times\left[(q_i^2-q^2)\left[\epsilon_0\frac{\omega^2}{c^2}-k_{\parallel}^2-q_i^2\right]+B\right]=0\ , \tag{20}$$

with $\mathrm{Im}q_i>0$. The particular q_i which makes the first square parentheses vanish, that we call q_3, is the wave vector of the longitudinal polariton, carrying zero magnetic field.

The relation between the x and z field components is obviously

$$\mathcal{E}_i^z=-(k_{\parallel}/q_i)\mathcal{E}_i^x\quad(i=1,2) \tag{21a}$$

for transverse waves, and

$$\mathcal{E}_3^z=(q_3/k_{\parallel})\mathcal{E}_3^x \tag{21b}$$

for the longitudinal wave ($i=3$). The substitution of (18) inside the original integro-differential system (12) yields two new conditions, which play the role of ABC's:

$$\sum_{i=1}^{3}\frac{\mathcal{E}_i^z}{q_i-q}-i\frac{\mathcal{E}_p^z}{P+iq}=2q\gamma/B\ , \tag{22a}$$

$$\sum_{i=1}^{3}\frac{\mathcal{E}_i^x}{q_i-q}-i\frac{\mathcal{E}_p^x}{P+iq}=2q\left[i\frac{\omega^2}{c^2}\eta-q\gamma\right]\Big/(k_{\parallel}B)\ . \tag{22b}$$

After a straightforward—but tedious—calculation, we explicitly find the electric field in the medium:

$$E_x(z)=\mathcal{E}_1^x\sum_{i=1}^{3}\gamma_i\left[\exp(iq_iz)+\frac{2P(P^2+q^2)}{(q_i^2-q^2)(P-iq_i)}\exp(-Pz)\right]\ , \tag{23a}$$

$$E_z(z)=\mathcal{E}_1^x\sum_{i=1}^{3}\bar{\gamma}_i\left[\exp(iq_iz)+\frac{2P(P^2+q^2)}{(q_i^2-q^2)(P-iq_i)}\exp(-Pz)\right]\ , \tag{23b}$$

$$\tilde{\gamma}_i=-k_{\parallel}\gamma_i/q_i \quad (i=1,2)\ , \tag{24a}$$

$$\tilde{\gamma}_3=q_3\gamma_3/k_{\parallel}\ , \tag{24b}$$

and

$$\gamma_1=1\ , \tag{25a}$$

$$\gamma_2\equiv\mathcal{E}_2^x/\mathcal{E}_1^x=-\frac{q_2(P-iq_2)(q_2^2-q^2)}{q_1(P-iq_1)(q_1^2-q^2)} \times\frac{B(P+iq_1)+2P(P^2+q^2)(P^2-k_{\parallel}^2+N^2)+\dfrac{BP}{N^2}(P+iq_1)^2-p_1p_4B/p_3}{B(P+iq_2)+2P(P^2+q^2)(P^2-k_{\parallel}^2+N^2)+\dfrac{BP}{N^2}(P+iq_2)^2-p_2p_4B/p_3}\ , \tag{25b}$$

$$\gamma_3\equiv\mathcal{E}_3^x/\mathcal{E}_1^x=\alpha_1+\alpha_2\gamma_2\ , \tag{25c}$$

with

$$N^2=\epsilon_0(\omega^2/c^2)-B/(P^2+q^2)\ , \tag{26}$$

$$p_4=P+iq_3+(2P/B)(P^2+q^2)(P^2-k_{\parallel}^2+N^2) +P(P+iq_3)(P-ik_{\parallel}^2/q_3)/N^2\ , \tag{27}$$

$$p_i/p_3=\frac{P+iq_i-\dfrac{2P}{B}(P^2+q^2)(k_{\parallel}^2-N^2+iPq_i)}{P+iq_3-\dfrac{2P}{B}(P^2+q^2)(k_{\parallel}^2-N^2+ik_{\parallel}P)} \quad (i=1,2)\ , \tag{28}$$

$$\alpha_i=\frac{(P-iq_3)(q_3^2-q^2)}{(P-iq_i)(q_i^2-q^2)}\frac{k_{\parallel}^2}{q_iq_3}\frac{p_i}{p_3} \quad (i=1,2)\ . \tag{29}$$

Finally the p-wave impedance becomes

$$Z_p\equiv E_x(0^+)/H_y(0^+)=-(k_{\parallel}c/\omega\epsilon_0)\frac{\sum_{i=1}^{3}\Gamma_i\gamma_i}{\sum_{i=1}^{3}\Gamma_i\tilde{\gamma}_i}\ , \tag{30}$$

where

$$\Gamma_i=1+2P(P^2+q^2)/[(q_i^2-q^2)(P-iq_i)]\ . \tag{31}$$

Through Maxwell's boundary conditions, namely the continuity of E_x, D_z, and H_y, we find the amplitude of the reflected wave

$$r_p=[-\omega Z_p(\omega,k_{\parallel})/c+k_z]/[\omega Z_p(\omega,k_{\parallel})/c+k_z]\ . \tag{32}$$

The limit $P\to\infty$ is of particular interest, because in this case the exciton wave function does not embody the evanescent wave $(1+A)\exp(-Pz)$. In this case it is simple to demonstrate that $\mathcal{E}_p^i$ vanishes as $P\to\infty$, and the result based on Pekar's ABC without dead layer is recovered. It should be emphasized that within our formulation the ABC's and the dead-layer depth are mutually dependent, so that only in the case of vanishing dead-layer Pekar's ABC's are recovered.

III. THEORY OF SURFACE POLARITONS AND ATR SPECTROSCOPY

It is well known that, in the absence of energy dissipation, Maxwell's equations admit surface electromagnetic waves—surface polaritons—with energy between $\hbar\omega_0$ and $\hbar\omega_L$.[11] The effect of the dead layer and spatial dispersion on surface polaritons has been investigated by many authors.[4,11–15] In this section we derive the dispersion relation and show how to compute ATR spectra, which are specially suited to detect surface polaritons, within the framework of the nonlocal dielectric function (1).

A. Surface polaritons

We assume that surface polaritons travel along the surface parallel to the x axis. The electric field is

$$E_\alpha(x,z,t)=E_\alpha(z)\exp(ik_{\parallel}x-i\omega t) \quad (\alpha=x,z)\ . \tag{33}$$

For the vacuum region ($z<0$) we seek solutions of the form

$$E_\alpha(z)=\mathcal{E}_\alpha^0\exp(\beta_0 z) \tag{34}$$

with β_0, real and positive, given by

$$\beta_0^2=k_{\parallel}^2-\omega^2/c^2\ . \tag{35}$$

Within the crystal ($z>0$) we search for solutions with the electric field

$$E_\alpha(z)=\sum_{i=1}^{3}\mathcal{E}_i^\alpha\exp(-\beta_i z)+\mathcal{E}_p^\alpha\exp(-Pz)\ . \tag{36}$$

The solution of Maxwell's equations for the surface polariton is the same as for the p wave, provided we replace q_i by $i\beta_i$ ($i=1,2,3$). We obtain two integro-differential equations similar to Eqs. (12). The β_i values are given by

$$[\epsilon_0(\beta_i^2+q^2)-B(c^2/\omega^2)] \left[(\beta_i^2+q^2)\left[\epsilon_0\frac{\omega^2}{c^2}-k_{\parallel}^2+\beta_i^2\right]-B\right]=0 \tag{37}$$

with $\mathrm{Re}(\beta_i)>0$.

A calculation formally similar to that of Sec. II B yields the impedance of surface waves:

$$Z_{\rm SW}=-(k_\parallel c/\epsilon_0\omega)\frac{\sum_{i=1}^{3}\gamma_i\left[1-\frac{2P(P^2+q^2)}{(\beta_i^2+q^2)(P+\beta_i)}\right]}{\sum_{i=1}^{3}\tilde{\gamma}_i\left[1-\frac{2P(P^2+q^2)}{(\beta_i^2+q^2)(P+\beta_i)}\right]} . \tag{38}$$

From the boundary conditions their dispersion relation becomes

$$Z_{\rm SW}(\omega,k_\parallel)=i\beta_0 c/\omega . \tag{39}$$

B. Attenuated total reflection

The observation of surface polaritons is usually performed by the attenuated total reflection (ATR) method, involving a transparent prism separated by an air or dielectric gap from the semiconductor. We adopt the same formalism as in Ref. 4. The electric field is

$$\mathcal{E}_\alpha(x,z,t)=E_\alpha(z)\exp(ik_\parallel x-i\omega t)\quad(\alpha=x,z) . \tag{40}$$

In the prism region (1), for $z<-d$, we write

$$E_z^{(1)}(z)=\exp(i\delta_1 z)+R\exp(-i\gamma_1 z) , \tag{41}$$

$$E_x^{(1)}(z)=\frac{\delta_1}{k_\parallel}(-e^{i\delta_1 z}+Re^{-i\delta_1 z}) , \tag{42}$$

where

$$\delta_1=\left[\epsilon_p\frac{\omega^2}{c^2}-k_\parallel^2\right]^{1/2}$$

and ϵ_p is the dielectric constant of the prism.

In the gap region (2), for $-d<z<0$, the electric field is

$$E_x^{(2)}(z)=A_1e^{-\delta_2 z}+A_2e^{\delta_2 z} , \tag{43}$$

$$E_z^{(2)}(z)=-k_\parallel(A_1e^{-\delta_2 z}-A_2e^{\delta_2 z})/(i\delta_2) , \tag{44}$$

where

$$\delta_2=\left[k_\parallel^2-\epsilon_g\frac{\omega^2}{c^2}\right]^{1/2}$$

and ϵ_g is the dielectric constant of the gap.

In the crystal (3), for $z>0$, we write

$$E_x^{(3)}(z)=\mathcal{E}_1^x\sum_{i=1}^{3}\gamma_i\left[e^{-\beta_i z}-\frac{2P(P^2+q^2)}{(\beta_i^2+q^2)(P+\beta_i)}e^{-Pz}\right] , \tag{45}$$

$$E_z^{(3)}(z)=\mathcal{E}_1^x\sum_{i=1}^{3}\tilde{\gamma}_i\left[e^{-\beta_i z}-\frac{2P(P^2+q^2)}{(\beta_i^2+q^2)(P+\beta_i)}e^{-Pz}\right] . \tag{46}$$

The boundary conditions at the prism-gap interface $z=-d$ and at the gap-semiconductor interface $z=0$ yield the reflectance amplitude in terms of the surface impedance $Z_{\rm SW}(k_\parallel,\omega)$:

$$R=\frac{\left[A_1^1+A_2^1-(A_1^1-A_2^1)\frac{\epsilon_g c}{\delta_2\omega}Z_{\rm SW}\right]}{\left[A_1^2+A_2^2-(A_1^2-A_2^2)\frac{\epsilon_g c}{\delta_2\omega}Z_{\rm SW}\right]} , \tag{47}$$

where

$$A_1^1=(i\delta_2\epsilon_p+\delta_1)\exp(-i\delta_1 d-\delta_2 d)/(2k_\parallel) , \tag{48a}$$

$$A_2^1=(\delta_1-i\delta_2\epsilon_p)\exp(i\delta_1 d-\delta_2 d)/(2k_\parallel) , \tag{48b}$$

$$A_1^2=(\delta_1-i\delta_2\epsilon_p)\exp(-i\delta_1 d+\delta_2 d)/(2k_\parallel) , \tag{48c}$$

$$A_2^2=(\delta_1+i\delta_2\epsilon_p)\exp(i\delta_1 d+\delta_2 d)/(2k_\parallel) . \tag{48d}$$

IV. DISCUSSION OF RESULTS

In this section we discuss and compare with experiments the results of calculations of exciton reflectance and ATR carried out according to the formulas of Secs. II and III. We want to address some issues: is our theory, based on the neglect of the image potential and of extrinsic dead layers, able to account for experiments? What is the difference between our calculations and those performed according to Pekar's ABC (with or without a homogeneous dead layer), to which our formulation is mostly similar? What would be the effect of a larger transition-layer depth, that might arise when the image potential is taken into account? Is there any experiment which might give a shortcut determination of such depth?

A. Normal-incidence reflectivity

In order to answer these questions, we first consider in Fig. 1(a) the normal-incidence reflectance of CdS, as measured in a high-purity sample,[16] where extrinsic effects should be very small. The correct normalization of the experimental result yields a peak reflectance of 0.51.[10] Our calculation, using a fixed value of the transition-layer depth, $1/P=18$ Å, resulting from the computed wave functions,[7] is in very good agreement with experiment, as already discussed in Ref. 10. The other parameters are taken from Brillouin scattering[17] and thin-film interference experiments.[18] Also shown in Fig. 1(a) are the results based on Pekar's ABC, with vanishing dead layer, and also our calculation carried out using a larger transition-layer depth, $1/P=50$ Å. This value roughly corresponds to $2a_B$, a widely used estimate of the dead-layer depth.[8,19] The curve based on Pekar's ABC is also in very good agreement with experiment, while that corresponding to $1/P=50$ Å has a similar line shape but a markedly different intensity and energy position. It is clear from these results that the line shape is poorly sensitive to the transition-layer depth, remaining unchanged from 0 up to the largest considered value, 50 Å. The comparison between our calculations and those based on the homogeneous dead-layer model is shown in Fig. 1(b). The curves corresponding to small dead layer ($d=18$ Å) and to the same value of the transition layer ($1/P=18$ Å)

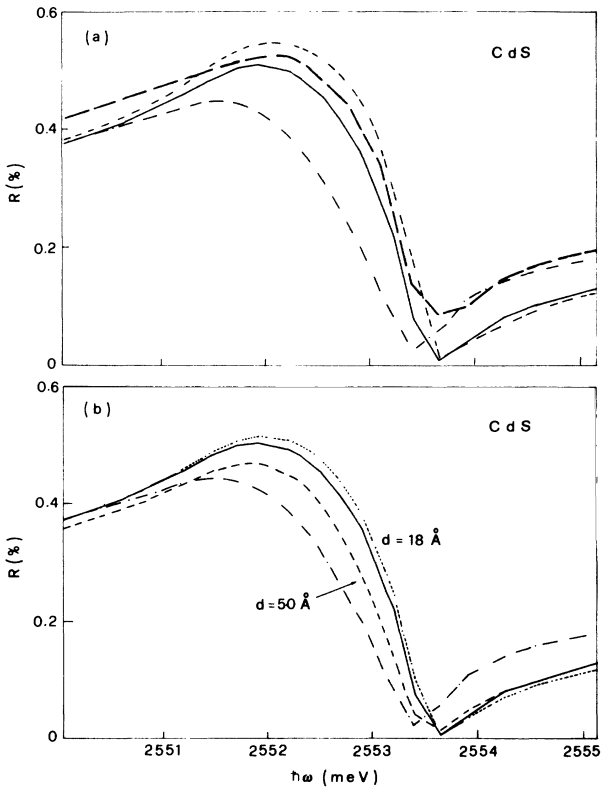

FIG. 1. Normal-incidence reflectance of the CdS A_1 exciton. (a) Comparison between experiment (long-dashed line, from Refs. 10 and 16) and theory; theoretical curves are computed using different values of the transition-layer depth $1/P$: 0 (short-dashed), 18 (solid) and 50 Å (dot-dashed line). (b) Comparison between our calculations [solid and dot-dashed lines, as in (a)] and those based on a homogeneous dead layer of depth d. Exciton parameters used in the calculations: $\hbar\omega_0=2.5525$ eV, $4\pi\alpha=0.013$, $\epsilon_0=8.1$, $M=0.94$, and $\Gamma=0.1$ meV.

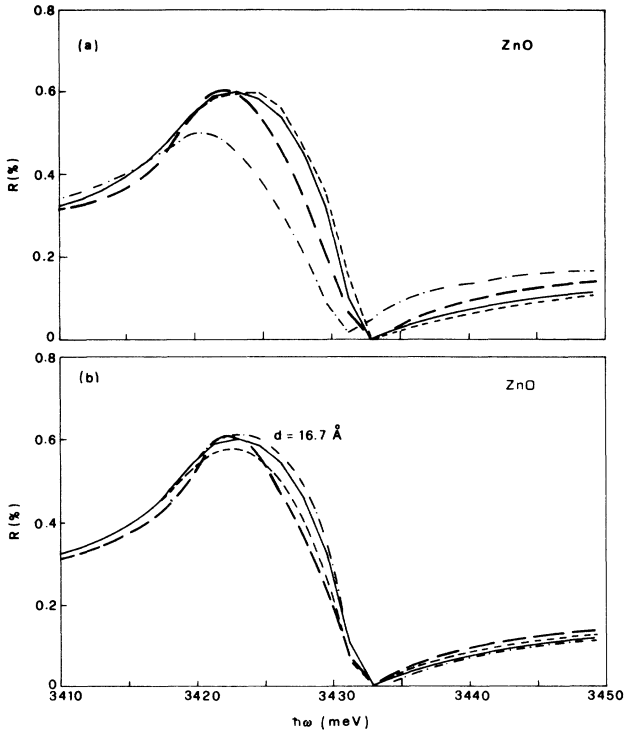

FIG. 2. Normal-incidence reflectance of the ZnO C_1 exciton. (a) Experiment from Ref. 20: long-dashed line; our calculations: short-dashed line ($1/P=0$), solid line ($1/P=11.6$ Å), and dot-dashed line ($1/P=35.8$ Å). (b) Experiment from Ref. 20: long-dashed line; our calculations: solid line ($1/P=11.6$ Å) and short-dashed line ($1/P=16.7$ Å); homogeneous dead-layer model for $d=16.7$ Å: dot-dashed line. Exciton parameters used in the calculations: $\hbar\omega_0=3.4198$ eV, $4\pi\alpha=0.043$, $\epsilon_0=6.2$, $M=0.83$, and $\Gamma=0.7$ meV.

are very similar, while the two approaches yield quite different results for larger depths ($d=1/P=50$ Å).

The normal-incidence experimental spectrum of the C_1 exciton in ZnO (Ref. 20) is shown in Fig. 2(a), together with the spectrum computed from wave functions ($1/P=11.6$ Å, solid line), that based on Pekar's ABC ($1/P=0$, short-dashed line), and that computed for $1/P$ equal to twice the exciton radius, i.e., 35.8 Å (dot-dashed line). The other parameters are taken from Ref. 20. Pekar's and our curves are very near each other, and in quite good agreement with the experimental spectrum. Both of them, however, present the same discrepancy with respect to experiment, namely too high reflectivity values between ω_0 and ω_L. This shortcoming was overcome in Ref. 20 by assuming, in addition to the dead layer, a surface-perturbed layer, where exciton parameters are different from bulk. It is interesting to learn whether our theory, involving an inhomogeneous transition layer, may account for the same effect. From inspection of Fig. 2(a) it seems that a larger depth of the transition layer, intermediate between 11.6 and 35.8 Å, may give a better agreement with experiment. This is indeed the case, since the curve computed for $1/P=16.7$ Å, which is compared with experiment in Fig. 2(b), is in better agreement with it. On the other hand, the homogeneous dead-layer approach, for $d=16.7$ Å, leads to a larger discrepancy with respect to experiment. We conclude that the inhomogeneous transition layer, characteristic of this model, is an essential ingredient to achieve quantitative agreement between experiment and theory in ZnO. The larger depth of such a layer (16.7 Å) with respect to that resulting from wave functions (11.6 Å) may be ascribed to the image potential, neglected in our model.

The normal-incidence reflectivity of InP, as measured by Mathieu *et al.*,[21] is shown in Fig. 3(a), together with theoretical curves corresponding to $1/P=0$ (Pekar's), 83.3 Å (computed from wave functions), and 238.1 Å ($2a_B$). The other parameters are taken from Refs. 5 and 22, with small changes made to reproduce the measured position of the dip, but without a least-squares fitting procedure. The agreement between experiment and our *ab initio* (i.e., from wave functions, $1/P=83.3$ Å) calculation is reasonably good. Pekar's curve is worse, while the assumption of a large transition layer, as deep as two exciton radii, yields a bad description of experiment. It may be of interest to see if the homogeneous

dead-layer approach gives better agreement. This can be seen in Fig. 3(b), where the curve computed for $d=238.1$ Å (homogeneous dead layer) is markedly different from the corresponding curve $1/P=238.1$ Å, and more similar to the experiment. The experiment is reasonably consistent with all considered values of the dead-layer depth, while it excludes the largest transition layer $1/P=238.1$ Å. However, the best agreement is with the curve computed for $d=238.1$ Å. In particular, the steep rise of the reflectivity above the minimum is well reproduced only by this curve. We conclude that there is evidence of a large ($\sim 2a_B$) homogeneous dead layer in InP.

In contrast with the materials considered so far, the reflectivity of GaAs (Ref. 23) is not well reproduced by the present theory, as already noted in Ref. 5. The feature which is not reproduced is the spike, often present in samples with low-quality surfaces.[23] The spike is largely reduced in good-quality samples,[23] and suppressed if the surface is cleaved in He atmosphere,[24] which is believed to minimize built-in electric fields near the surface. In this case the spike changes into a steplike rise of reflectance just above ω_L, which is by no means reproduced by our theory, as can be seen in Fig. 4. The theoretical curves are for $1/P=0$ (Pekar's), 65 Å (from wave functions), and 222 Å ($2a_B$). On the other hand, the steplike rise has been well reproduced by the adiabatic two-parameter calculation of Balslev.[24,25] In this case, one of the parameters, d, is related to the length of exponential decay of the potential acting on the exciton center of mass, while the other one, z_0, moves the position of the surface barrier with respect to the surface. Roughly speaking, d is similar to our P^{-1}, while z_0 simulates the effect of a homogeneous dead layer. The large value of z_0 (440 Å) used in Ref. 25 suggests that a large homogeneous dead layer can also give a good account of experiment. We can see from Fig. 3(b) that this conjecture is probably correct, since in the case of InP (largely similar to GaAs) the curve computed for $d=238.1$ Å shows the correct steplike rise on the high-energy side. These findings address the question of the failure of our microscopic calculations to describe exciton reflectivity line shapes of the very similar semiconductors InP and GaAs. In view of such similarity, we believe that the origin of the failure should be intrinsic. It might be due to the image potential or to band degeneracy: both of these aspects have been neglected in our calculation.

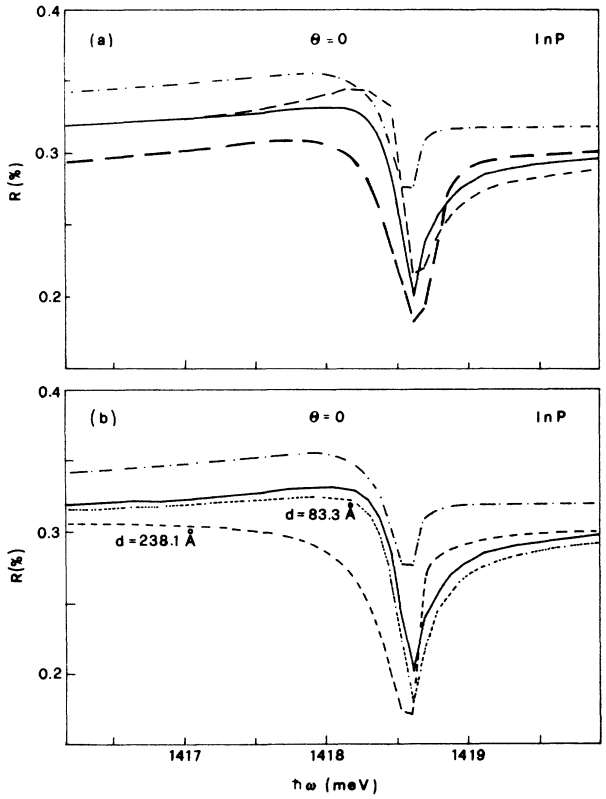

FIG. 3. Normal-incidence reflectance of the lowest-energy exciton in InP. (a) Experiment from Ref. 21: long-dashed line; our calculations: short-dashed line ($1/P=0$), solid line ($1/P=83.3$ Å), and dot-dashed line ($1/P=238.1$ Å). (b) Our calculations: solid and dot-dashed lines as in (a); homogeneous dead-layer model: dotted line ($d=83.3$ Å) and short-dashed line ($d=238.1$ Å). Exciton parameters used in the calculations: $\hbar\omega_0=1.4183$ eV, $4\pi\alpha=0.31\times10^{-2}$, $\epsilon_0=12.1$, $M=0.25$, and $\Gamma=0.02$ meV.

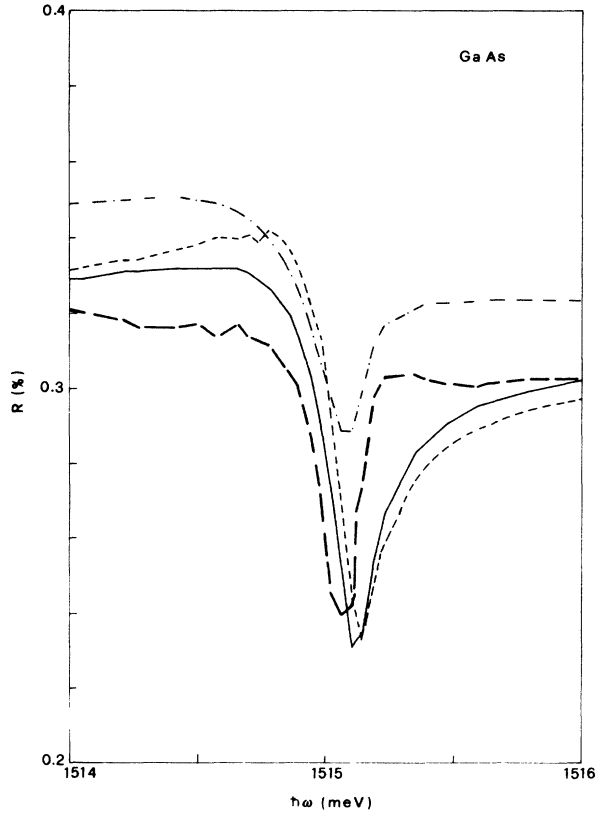

FIG. 4. Normal-incidence reflectance of the lowest-energy exciton in GaAs. Experiment from Ref. 24: long-dashed line. Our calculations: short-dashed line ($1/P=0$), solid line ($1/P=65$ Å), and dot-dashed line ($1/P=222$ Å). Exciton parameters used in the calculations: $\hbar\omega_0=1.515$ eV, $4\pi\alpha=0.22\times10^{-2}$, $\epsilon_0=12.6$, $M=0.298$, and $\Gamma=0.035$ meV.

Finally we consider in Fig. 5 the normal-incidence reflectivity of ZnTe, measured by Brodin *et al.*[26] on vapor-grown samples. We also show theoretical curves for $1/P=0$ (Pekar's), 41.6 Å (from wave functions), and 120.5 Å ($2a_B$). The other parameters are taken from the literature,[27–29] with some changes meant to reproduce oblique-incidence reflectance,[30] as explained later on. Pekar's and our *ab initio* calculation give reasonable agreement. Much better agreement can be obtained by changing ω_0 and Γ a little bit with respect to the parameters used for the non-normal incidence case, which can be understood since the normal- and oblique-incidence spectra have been taken by different groups on different samples.[26,30] However, since the aim of this work is not to give the best fit of each experiment, but rather a reasonable description of many experiments using the same set of parameters, we do not show these spectra.

Including the case of ZnSe, already treated in Ref. 5, we may say that our theory gives a good description of normal-incidence reflectance in several semiconductors. Pekar's ABC also gives a reasonable description in the same cases, while there is no evidence of large ($\sim 2a_B$) transition layers. A large homogeneous dead layer seems to be involved in the case of GaAs and InP.

B. Oblique-incidence reflectivity

Let us first consider the *p*-wave reflectance of CdS, as measured by Broser *et al.*[31] on a good-quality sample, i.e., selected not to show spikes at ω_L. The agreement between our theory ($1/P=18$ Å) and experiment is very good (see Fig. 6), as was already noticed in Ref. 10. No *ad hoc* change of parameters has been introduced with respect to normal-incidence reflectivity, except increasing $\hbar\omega_0$ by 1 meV, which takes into account possible different absolute calibrations of the frequency scale in the two-experiments, carried out by two different groups. The curves computed for Pekar's case and for $1/P=50$ Å are also shown in Fig. 6. Pekar's theory seems to work better at large angles. The effect of the transition layer appears to be more important at [Fig. 6(c)] and above [Fig. 6(d)] the Brewster angle. It is interesting to notice that just at the Brewster angle a homogeneous dead layer has no effect on *p*-wave reflectance. We may conclude that this measurement makes the difference between our theory, working well at all angles, and that of Pekar. Broser *et al.* have also shown the reflectance of a lower-quality sample, with well-pronounced spikes at several incidence angles. Of course these spectra are not in agreement with ours, not only for the presence of the spikes, but also for weaker exciton reflectance as a general trend. The same trend and spikes are observed in other *p*-reflectance measurements by Stössel and Wagner.[32] The arguments discussed above lead to the conclusion that the sample used in this case is of low quality, i.e., it has an extrinsic dead layer.

The only measurement of *s*-wave reflectance in CdS of which we know, is that carried out by Stössel and

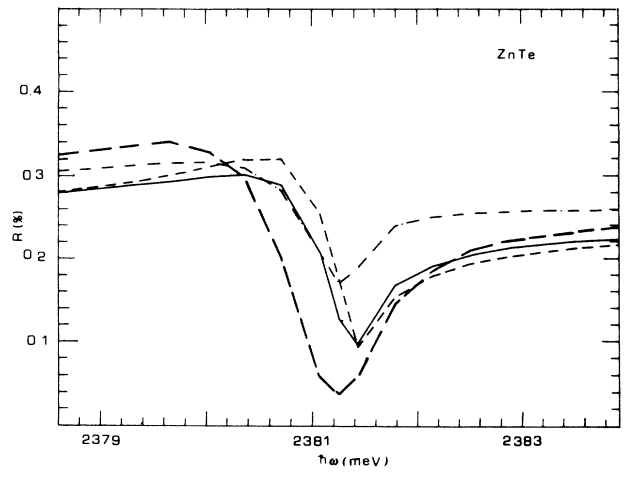

FIG. 5. Normal-incidence reflectance of the lowest-energy exciton in ZnTe. Experiment from Ref. 26: long-dashed line. Our calculations: short-dashed line ($1/P=0$), solid line ($1/P=41.6$ Å), and dot-dashed line ($1/P=120.5$ Å). Exciton parameters used in the calculations: $\hbar\omega_0=2.3808$ eV, $4\pi\alpha=0.0045$, $\epsilon_0=8.7$, $M=0.38$, and $\Gamma=0.08$ meV.

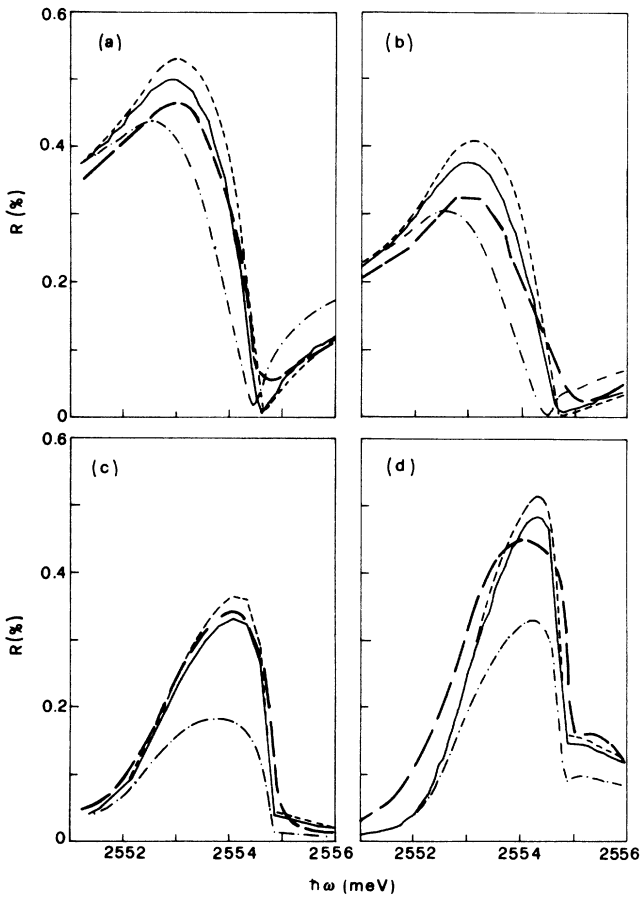

FIG. 6. *p*-wave reflectance of the A_1 exciton in CdS at various angles of incidence: 11° (a), 48° (b), 71° (c), and 78° (d). Experiment from Ref. 31 (sample B-109): long-dashed lines. Our calculations: short-dashed lines ($1/P=0$), solid lines ($1/P=18$ Å), and dot-dashed lines ($1/P=50$ Å). Exciton parameters as in Fig. 1, except that $\hbar\omega_0=2.5525$ eV.

Wagner on the same sample mentioned above.[32] The agreement with theory (see Fig. 7) is worse than that of Fig. 6. As a general trend, the experimental structures are weaker than theoretical ones, computed for small transition layers. The large transition-layer curve is in better agreement with experiment than the other ones. In view of the discussion above, we ascribe this feature to the presence of a large extrinsic dead layer at the surface.

The measurements of s- and p-wave reflectance of ZnTe, carried out by Pevtsov and Sel'kin[30] at 45° and 82°, are compared with theory in Fig. 8. Theoretical curves are computed for $1/P=0$ (Pekar's), 41.7 Å (from wave functions), and 120.5 Å ($2a_B$). The exciton parameters, quoted in the figure caption, are taken from the literature,[27–30] with some changes necessary to give a reasonable description of non-normal incidence experiments. The agreement with theory is only qualitative. The general trend of weaker experimental than computed structures points toward a bad-quality sample as the reason of the discrepancy. However, it must also be taken into account that we have not performed a least-squares fitting procedure in order to determine the exciton parameters,

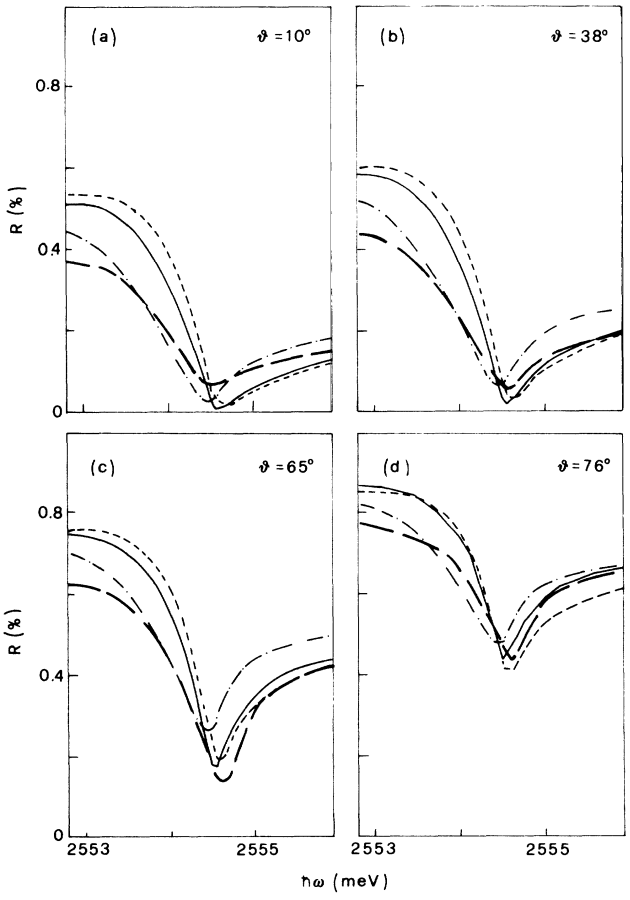

FIG. 7. s-wave reflectance of the A_1 exciton in CdS at various angles of incidence ϑ. Drawing of curves and exciton parameters as in Fig. 6. Different values of the exciton mass in the direction parallel ($M_{\parallel}=2.4$) and perpendicular ($M_{\perp}=0.94$) to the surface have been used in the calculations. Experiment from Ref. 32.

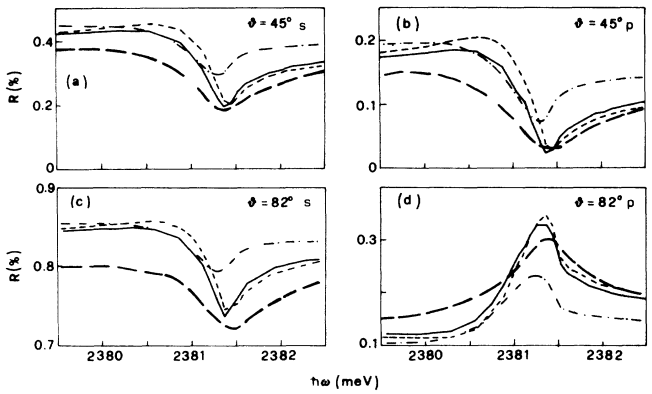

FIG. 8. s- and p-wave reflectance of the lowest-energy exciton in ZnTe, for two angles, of incidence: $\vartheta=45°$ and 82°. Experiment from Ref. 30: long-dashed lines. Our calculations: short-dashed lines ($1/P=0$), solid lines ($1/P=41.6$ Å), and dot-dashed lines ($1/P=120.5$ Å). Exciton parameters as in Fig. 5.

which is especially relevant in view of the spread of the values quoted in the literature.[26–30]

C. Phase of the reflected light

Recently Gotthard[33] has suggested measuring the reflectance of circularly polarized light in order to detect the phase difference of the reflected p and s waves. Such a difference has been shown to be quite sensitive to the ABC. Here we want to investigate whether the phase difference is a good check also of the transition-layer depth. We have computed the phase difference from Eqs. (10) and (32), and compared the result with experiment when available.

First we consider in Fig. 9 the phase difference measured by Pevtsov and Sel'kin on ZnTe,[30] using the same sample of Fig. 8. Theoretical curves have been computed using the same parameters and P values as in Fig. 8. We see that the difference between our ($1/P=41.7$ Å) and Pekar's calculations is quite small, while the large transition-layer ($1/P=120.5$ Å) curve is markedly different. Experimental data are quite well described by the latter. This cannot be taken, however, as definite evidence of the presence of a large intrinsic transition layer, because the normal-incidence reflectance computed using a large transition layer is not in agreement with experiment (see Fig. 5).

The phase difference of reflected p and s waves has been measured also in CdS by Pevtsov *et al.*[34] at an angle of incidence of 8°. In the geometry considered by Pevtsov *et al.* the electric field of the s wave is parallel to the c axis, so that it does not excite the A exciton, which is only allowed for polarization perpendicular to the c axis.[31,32] As a consequence, the phase of the reflected s wave is constant, as far as the background dielectric constant ϵ_0 does not vary. The frequency dependence of the measured phase difference actually follows the phase of the p reflected wave. This has been computed using the same values of parameters as in Figs. 1, 6, and 7. The results, plotted in Fig. 10, are in reasonable agreement with

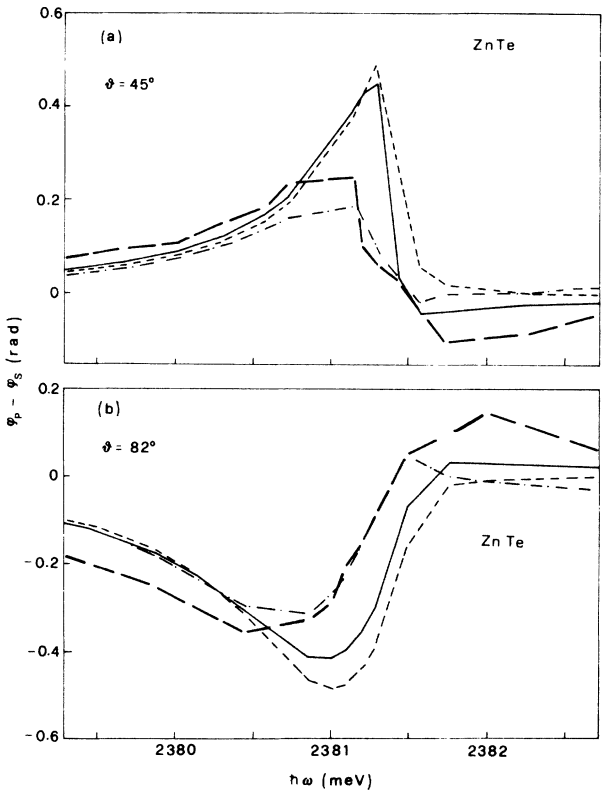

FIG. 9. Phase difference of reflected p and s waves near the lowest-energy exciton in ZnTe, for two angles of incidence: $\vartheta=45°$ and 82°. Drawing of curves and exciton parameters as in Fig. 8. Experiment from Ref. 30.

experiment. Again our curve and Pekar's curve are very similar.

The phase difference has also been computed for the case of InP, in order to check if the effect of the transition layer is larger in the case of weakly bound large-radius excitons, as those of InP. The results are plotted in Fig. 11. Actually the large transition-layer ($2a_B$) curve has a peculiar feature, namely the sharp peak on the high-frequency side.

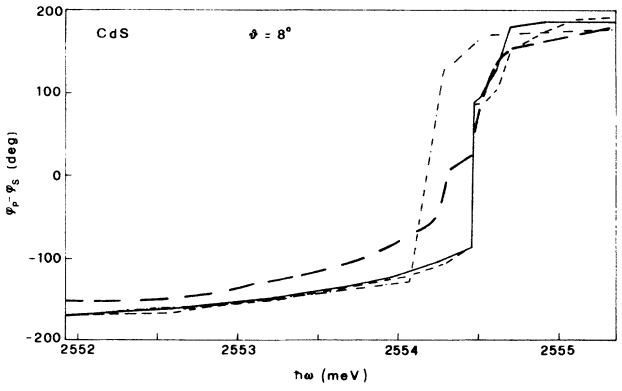

FIG. 10. Phase difference of reflected p and s waves near the A_1 exciton in CdS, for an angle of incidence of 8°. Experiment from Ref. 34: long-dashed line. Our calculations: curves and exciton parameters as in Figs. 6 and 7.

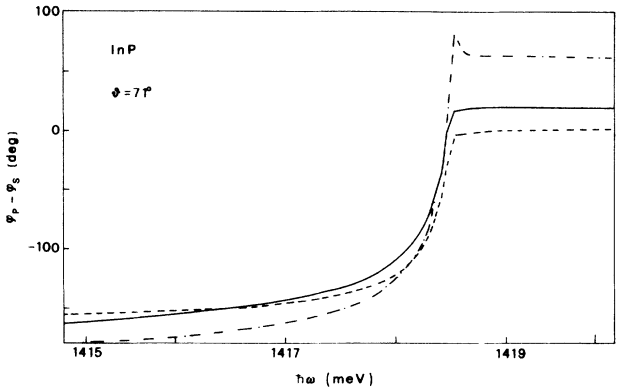

FIG. 11. Phase difference of reflected p and s waves near the lowest-energy exciton in InP. The curves have been computed using $1/P=0$ (dashed), 83.3 (solid), and 238.1 Å (dot-dashed line) and the same exciton parameters as in Fig. 3.

D. Attenuated total reflection and surface polaritons

The ability to give a good description of ATR spectra is a crucial test of any theory of exciton polaritons. For instance, the ATR spectrum of the C_1 exciton in ZnO is not well described for any choice of the parameter U, defined in Ref. 3, which is related to the ABC.[3] Here we do not attempt to discuss this case, since the solution of Maxwell's equations reported in Sec. III—because of the assumed isotropy in the plane of incidence—cannot be applied to the anisotropic experimental geometry.[35,36] We discuss, however, the case of the cubic semiconductor ZnSe, whose ATR spectra have been measured by Tokura *et al.*[37]

The fair agreement between our calculations and experiment at various angles of incidence has already been noticed in Ref. 10. Here we discuss the sensitivity of calculated spectra to the ABC and to the transition-layer depth. The experimental and computed ATR spectra corresponding to $1/P=0$ (Pekar's), 24.4 Å (from wave functions), and 80 Å ($2a_B$) are shown in Fig. 12, for an angle of incidence of 68.5°. The experimental minimum is reasonably well described by our and Pekar's theories, while the large transition-layer curve leads to a weaker structure. Similar results are obtained for the other angles of incidence shown in Fig. 4 of Ref. 10. The positive experimental peak on the high-frequency side is so far unexplained.[37] It might be related to the splitting between heavy and light excitons that occurs in cubic crystals.

E. Polariton population

Recently some experiments[38] have detected in CuCl optical transitions, in the presence of an exciting laser beam, from the upper- and lower-polariton branches to the exciton molecule. The measured intensity ratio can be related to the different populations of the two branches, mainly determined by the ABC. These experiments could be, therefore, a powerful test of the ABC. Since in our theory the transition-layer depth and ABC

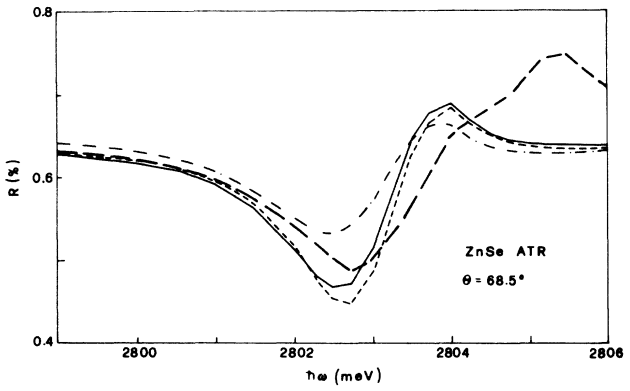

FIG. 12. ATR in ZnSe at an incidence angle of 68.5°. Experiment from Ref. 37: long-dashed line. Our calculations: short-dashed line ($1/P=0$), solid line ($1/P=24.4$ Å), and dot-dashed line ($1/P=80$ Å). Exciton parameters used in the calculation: $\hbar\omega_0=2.802$ eV, $4\pi\alpha=0.88\times10^{-2}$, $\epsilon_0=8.1$, $M=0.6$, and $\Gamma=0.4$ meV. Prism and gap parameters: $\epsilon_p=2.634$; $\epsilon_g=1.769$; gap depth is 1000 Å.

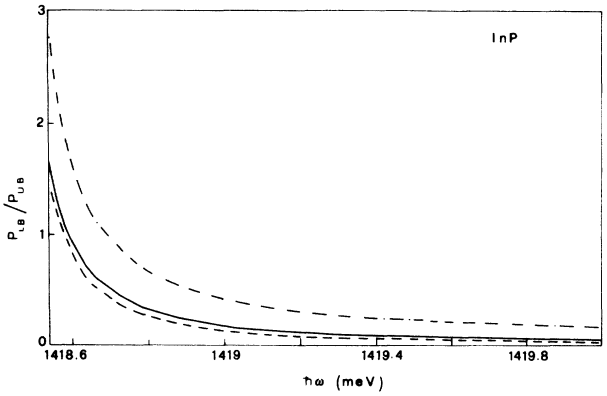

FIG. 14. Relative population of the lower-polariton branch to the upper-polariton branch, calculated for InP, using $1/P=0$ (dashed line), 83.3 Å (solid line), and 238.1 Å (dot-dashed line). Exciton parameters as in Fig. 3.

are related, they can also check the value of P. The first interpretation of the experiment[38] was against all postulated ABC's. A later reconsideration[39] of the experimental (slab) geometry pointed out, however, that the different escape probabilities from the back surface of the two polariton branches should be taken into account. In our formulation, this implies that one should compute polariton populations in a finite slab, which is beyond the purpose of this work. Therefore we will not attempt to compare our results with experiment. We want, however, to investigate how sensitive the population ratio is to the value of P. This is done looking at Figs. 13 and 14, where the ratio of polariton populations, induced by light normally incident on semi-infinite CuCl and InP samples, respectively, is plotted. (The population of a branch is taken proportional to its group velocity times the square of its polarization, as in Ref. 38.) The most interesting feature is that the population is indeed sensitive to the P value. On the contrary, in the case of a homogeneous dead layer, it does not depend on its depth, but only on the ABC. The possibility of experimental detection of the transition-layer effect is, however, limited to large depths, of the order of $2a_B$.

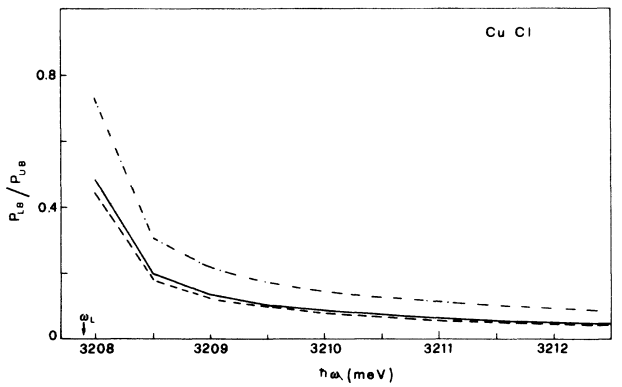

FIG. 13. Relative population of the lower-polariton branch to the upper-polariton branch calculated for CuCl, for $1/P=0$ (dashed line), 5 Å (solid line), and 13.5 Å (dot-dashed line). Exciton parameters used in the calculation: $\hbar\omega_0=3.2022$ eV, $4\pi\alpha=0.02$, $\epsilon_0=5.6$, $M=2.3$, and $\Gamma=0.01$ meV.

V. CONCLUSION

In this section we try to summarize the results of this work, that is, to answer the questions addressed in the Introduction.

Our microscopic theory gives, basically without adjustable parameters, a fairly good account of many experiments carried out on good-quality samples of most materials, namely CdS, ZnO, ZnSe, and ZnTe. It does not succeed in describing the normal-incidence reflectance line shape of excitons in GaAs and partially in InP, and the oblique-incidence reflectance amplitude in ZnTe.

We believe that the ZnTe failure is due to the presence of deep extrinsic dead layers in the sample on which the measurements have been carried out. The good agreement found for the normal-incidence reflectivity and the type of discrepancies between theory and experiment found in oblique-incidence reflectivity, carried out on a different sample, suggest that the discrepancies should be ascribed to the low quality of this sample.

The case of GaAs is more difficult to explain on this ground, since the measurement[24] was carried out on a sample cleaved in helium atmosphere to avoid surface electric fields. The discrepancy between experiment and theory might be due to a failure of the latter to take into account the image potential as well as band degeneracy, which occurs in cubic crystals. A good description of the experiment is instead given by a fairly large ($2a_B$) homogeneous dead layer. The similarity of exciton parameters between GaAs and InP,[5] and the very fact that the reflectivity of the latter shows a similar—yet smaller—discrepancy with respect to theory, points to an intrinsic

origin[2] of the homogeneous dead layers in both crystals.

The differences between our calculations, where the transition-layer depth is computed from wave functions, and those based on Pekar's ABC (without dead layer) are surprisingly small, in view of the fact that the parameter U in (1), i.e., the weight of the specularly reflected term, is quite different in the two cases,[10] for instance when ATR is considered. However, the detailed comparison between theory and experiment can sometimes make a choice between them: for instance, our calculations well describe CdS p-wave reflectance at all angles of incidence, while Pekar's do not.

In general, the computed curves are weakly sensitive to the values of the transition-layer depth. Clearcut differences are present only between small depths ($<a_B$) and large depths ($\sim 2a_B$). Large transition layers were indeed always excluded by the experiment, except for the s-p phase difference in ZnTe. In the case of ZnO (see Fig. 2) a detailed comparison between theory and experiment determines the transition-layer depth with great accuracy: this happens because theory gives a very good description of this experiment. The value of $1/P$ found in this way is a little bit larger than the computed one: this can be explained as an effect of the image potential, which has been neglected in the calculation. The case of ZnO points out the importance of the specific effects of the inhomogeneous transition layer, which were previously described by means of an additional surface layer, where excitons have different properties than in bulk.[20]

The differences between reflectivity curves computed according to the present formulation, i.e., involving a transition layer of depth $1/P$, and those computed for the case of a homogeneous dead layer of the same depth $d=1/P$, are small for small values of d, i.e., $d<a_B$. For large d, i.e., for $d\simeq 2a_B$, larger differences are present. In the case of large radius excitons, e.g., in InP and GaAs, the large transition-layer curves are qualitatively different from small transition-layer curves, while the homogeneous dead-layer model for $d=2a_B$ yields results which are qualitatively similar to that corresponding to $d=0$ [see Fig. 3(b)], and in good agreement with experiment. Only for $d>2a_B$ an extra feature, the spike, appears in the line shape. We summarize this situation saying that experiments are weakly sensitive to the dead-layer depth. This is the reason, together with the inaccurate determination of the absolute reflectivity in the case of CdS,[10] for the large estimates of d resulting from curve fitting, even in the case of good-quality samples[3,20,31,40] of materials for which the small-transition-layer calculations presented here give a good description of experiments. In the case of InP and GaAs a large dead layer is absolutely needed in order to reproduce some features of experimental spectra.

We want finally to point out the ability of the present approach to derive—basically without approximations—analytical formulas relevant for a number of experimental arrangements, from the exact (numerical) wave functions of a microscopic model.[7] All approximations are embodied in the model, while the calculation is carried out basically without introducing further approximations. Such ability, together with the good agreement found in several cases between theory and experiment, strongly encourages its extension to embodying the aspects which have been neglected so far, for instance the image potential and band degeneracy, and to other geometries, for instance to the case of a slab.[41]

[1] S. I. Pekar, Zh. Eksp. Teor. Fiz. **33**, 1022 (1957) [Sov. Phys.—JETP **6**, 785 (1958)].

[2] J. J. Hopfield and D. G. Thomas, Phys. Rev. **132**, 563 (1963).

[3] P. Halevi and G. Hernandez-Cocoletzi, Phys. Rev. Lett. **48**, 1500 (1982), and references therein.

[4] A. A. Maradudin and D. L. Mills, Phys. Rev. B **6**, 2787 (1973).

[5] A. D'Andrea and R. Del Sole, Phys. Rev. B **25**, 3714 (1982).

[6] M. Altarelli, G. B. Bachelet, V. Bouché, and R. Del Sole, Surf. Sci. **129**, 447 (1983).

[7] A. D'Andrea and R. Del Sole, Phys. Rev. B **32**, 2337 (1985).

[8] I. Balslev, Phys. Status Solidi B **88**, 155 (1978).

[9] S. Sakoda, J. Phys. Soc. Jpn. **40**, 152 (1976).

[10] A. D'Andrea and R. Del Sole, Phys. Rev. B **29**, 4782 (1984).

[11] B. Fischer and H. J. Queisser, Solid State Commun. **16**, 1125 (1975).

[12] P. R. Rimbey, Phys. Status Solid B **68**, 617 (1975).

[13] J. Lagois and B. Fischer, Phys. Rev. Lett. **36**, 680 (1976).

[14] J. Lagois and B. Fischer, Solid State Commun. **18**, 1519 (1976).

[15] M. Fukui, V. C. Y. So, and G. I. Stegeman, Solid State Commun. **30**, 683 (1979).

[16] F. Evangelisti, A. Frova, and F. Patella, Phys. Rev. B **10**, 1253 (1974).

[17] P. Yu and F. Evangelisti, Phys. Rev. Lett. **42**, 1642 (1979).

[18] J. Voigt, M. Senoner, and J. Ruckmann, Phys. Status Solidi B **75**, 231 (1976).

[19] F. Evangelisti, J. U. Fischback, and A. Frova, Phys. Rev. B **9**, 1516 (1974).

[20] J. Lagois, Phys. Rev. B **10**, 5511 (1981).

[21] H. Mathieu, Y. Chen, J. Camassel, and J. Allegre, Phys. Rev. B **32**, 4042 (1985).

[22] A. D'Andrea and R. Del Sole, Solid State Commun. **30**, 145 (1979).

[23] D. D. Sell, S. E. Stokowski, R. Dingle, and J. V. Di Lorenzo, Phys. Rev. B **7**, 4568 (1973).

[24] L. Schultheis and I. Balslev, Phys. Rev. B **28**, 2292 (1983).

[25] I. Balslev, Solid State Commun. **39**, 359 (1981).

[26] M. S. Brodin, V. M. Bandura, and M. G. Matsko, Phys. Status Solidi B **125**, 613 (1984).

[27] H. Venghaus, B. Jusserand, and G. Behnke, Solid State Commun. **33**, 371 (1980).

[28] H. Venghaus and B. Jusserand, Phys. Rev. B **22**, 932 (1980).

[29] M. S. Brodin and M. G. Matsko, Solid State Commun. **35**, 375 (1980).

[30] A. B. Pevtsov and A. V. Sel'kin, Fiz. Tverd. Tela (Leningrad) **23**, 2814 (1981) [Sov. Phys.—Solid State **23**, 1644 (1981)].

[31] I. Broser, M. Rosenzweig, R. Broser, M. Richard, and E. Birkicht, Phys. Status Solidi B **90**, 77 (1978).

[32] W. Stössel and H. J. Wagner, Phys. Status Solidi B **89**, 403 (1978); **96**, 369 (1979).

[33]L. Gotthard, Solid State Commun. **51**, 975 (1984).
[34]A. B. Pevtsov, S. A. Permogorov, Sh. R. Saifullaev, and A. V. Sel'kin, Fiz. Tverd. Tela (Leningrad) **22**, 2400 (1980) [Sov. Phys.—Solid State **22**, 1396 (1980)].
[35]J. Lagois and K. Hummer, Phys. Status Solidi B **72**, 393 (1975).
[36]J. Lagois, Solid State Commun. **39**, 563 (1981).
[37]Y. Tokura, T. Koda, I. Hirabayashi, and S. Nakada, J. Phys. Soc. Jpn. **50**, 145 (1981).
[38]Y. Segawa, Y. Ayogi, S. Komuro, and S. Namba, Phys. Rev. Lett. **50**, 43 (1983).
[39]E. Hanamura, Solid State Commun. **51**, 213 (1984).
[40]F. Patella, F. Evangelisti, and M. Capizzi, Solid State Commun. **20**, 23 (1976).
[41]A. D'Andrea and R. Del Sole, in *Excitons in Confined Systems,* edited by R. Del Sole, A. D'Andrea, and A. Lapiccirella (Springer-Verlag, Berlin, 1988), p. 102.